

This discussion paper is/has been under review for the journal Biogeosciences (BG).
Please refer to the corresponding final paper in BG if available.

How significant is submarine groundwater discharge and its associated dissolved inorganic carbon in a river-dominated shelf system-the northern South China Sea?

Q. Liu¹, M. Dai^{1,*}, W. Chen^{1,2}, C.-A. Huh², G. Wang¹, Q. Li¹, and M. A. Charette³

¹State Key Laboratory of Marine Environmental Science, Xiamen University, Xiamen, China

²Institute of Earth Sciences, Academia Sinica, Taipei, China

³Department of Marine Chemistry and Geochemistry, Woods Hole Oceanographic Institution, Woods Hole, MA, USA

Received: 14 November 2011 – Accepted: 22 November 2011

– Published: 21 December 2011

Correspondence to: M. Dai (mdai@xmu.edu.cn)

Published by Copernicus Publications on behalf of the European Geosciences Union.

**How significant is
submarine
groundwater
discharge?**

Q. Liu et al.

Title Page

Abstract

Introduction

Conclusions

References

Tables

Figures

⏪

⏩

◀

▶

Back

Close

Full Screen / Esc

Printer-friendly Version

Interactive Discussion

Abstract

In order to assess the role of submarine groundwater discharge (SGD) and its impact on the carbonate system on the northern South China Sea (NSCS) shelf, we measured seawater concentrations of four radium isotopes $^{223,224,226,228}\text{Ra}$ along with carbon dioxide parameters in June–July, 2008. Complementary groundwater sampling was conducted in coastal areas in December 2008 and October 2010 to constrain the groundwater end-members. The distribution of Ra isotopes in the NSCS was largely controlled by the Pearl River plume and coastal upwelling. Long-lived Ra isotopes (^{228}Ra and ^{226}Ra) were enriched in the river plume but low in the offshore surface water and subsurface water/upwelling zone. In contrast, short-lived Ra isotopes (^{224}Ra and ^{223}Ra) were elevated in the subsurface water/upwelling zone as well as the river plume but depleted in the offshore surface water. In order to quantify SGD, we adopted two independent mathematical approaches. Using a three end-member mixing model with total alkalinity (TAlk) and Ra isotopes, we derived a SGD flux into the NSCS shelf of $2.3\text{--}3.7 \times 10^8 \text{ m}^3 \text{ d}^{-1}$. Our second approach involved a simple mass balance of ^{228}Ra and ^{226}Ra and resulted in a first order but consistent SGD rate estimate of $2.8\text{--}4.5 \times 10^8 \text{ m}^3 \text{ d}^{-1}$. These fluxes were equivalent to 13–25 % of the Pearl River discharge, but the source of the SGD is mostly recirculated seawater. Despite the relatively small SGD volume flow compared to the river, the associated material fluxes were substantial given the elevated concentrations of dissolved inorganic solutes. In this case, dissolved inorganic carbon (DIC) flux through SGD was $266\text{--}520 \times 10^9 \text{ mol yr}^{-1}$, which was $\sim 44\text{--}73\%$ of the riverine DIC export flux. Given our estimates of the groundwater-derived phosphate flux, SGD may be responsible for new production on the shelf up to $3\text{--}6 \text{ mmol C m}^{-2} \text{ d}^{-1}$. This rate of new production would at most consume 18 % of the DIC contribution delivered by SGD. Hence, SGD may play an important role in the carbon balance over the NSCS shelf.

How significant is submarine groundwater discharge?

Q. Liu et al.

Title Page

Abstract

Introduction

Conclusions

References

Tables

Figures



Back

Close

Full Screen / Esc

Printer-friendly Version

Interactive Discussion



1 Introduction

Recent studies have recognized SGD as an important component of the hydrological cycle and chemical budgets in the coastal zone (Swarzenski et al., 2001; Taniguchi et al., 2002; Burnett et al., 2003; Charette et al., 2003; Moore, 2003; Bokuniewicz et al., 2008). Moore et al. (2008) estimated that the SGD flux to the Atlantic Ocean is similar in volume to the riverine flux. SGD is often characterized by very high concentrations of nutrients, trace metals, inorganic carbon, and organic matter as compared with surface water. Inputs of these materials can have a profound impact on the biogeochemistry and ecosystem functioning of coastal systems (Moore, 2010a). In particular, SGD has been shown to be an important nutrient source to estuaries, salt marshes, oceanic islands, and coral reefs (Marsh, 1977; Johannes, 1980; Capone and Bautista, 1985; Charette and Buesseler, 2004; Charette, 2007; Santos et al., 2008; Burnett et al., 2009; Garcia-Solsona et al., 2010; Kim et al., 2011). As a consequence, studies have proposed a linkage between SGD and coastal eutrophication and harmful algae bloom outbreaks (Hu et al., 2006; Lee and Kim, 2007; Lee et al., 2010). Cai et al. (2003) reported extremely high partial pressure of CO_2 ($p\text{CO}_2$) and DIC in coastal wells along South Carolina, US and they estimated that the DIC flux associated with SGD to these coastal waters was comparable to the contribution of nearby river systems.

While it is clear that many coastal systems are impacted by SGD, its influence on river-dominated ocean margins (RioMar) is less well known, mainly because material inputs from river plumes are substantial and mixing between different fluid sources is often complex. One of the challenges is that river plumes very often possess the same geochemical signals as SGD. While studies in the Mississippi, Atchafalaya, and Chao Phraya estuaries using Ra isotopes (Krest et al., 1999; Moore and Krest, 2004; Dulaiova and Burnett, 2006) have already suggested its overall importance, quantitative SGD estimates remain difficult in these systems.

The NSCS is a major river-dominated shelf margin (Dagg et al., 2008). The strong river plume is generated from the Pearl River, which is typically transported eastward

BGD

8, 12381–12422, 2011

How significant is submarine groundwater discharge?

Q. Liu et al.

Title Page

Abstract

Introduction

Conclusions

References

Tables

Figures



Back

Close

Full Screen / Esc

Printer-friendly Version

Interactive Discussion

**How significant is
submarine
groundwater
discharge?**

Q. Liu et al.

[Title Page](#)[Abstract](#)[Introduction](#)[Conclusions](#)[References](#)[Tables](#)[Figures](#)[⏪](#)[⏩](#)[◀](#)[▶](#)[Back](#)[Close](#)[Full Screen / Esc](#)[Printer-friendly Version](#)[Interactive Discussion](#)

widening and thickening buoyant plume over the shelf in summer (Gan et al., 2009b). The surface sediments across the NSCS continental shelf show grain size gradations, from gravel inshore to silt offshore. The sediments consist of both terrigenous and biogenous detritus, as well as small amounts of authigenic minerals (Luo et al., 1985; Zhang et al., 2003). The region along the shoreline of the NSCS is composed of thick and widespread Quaternary deposits (Chen, 2008). The delta plain is formed by thick sediments of alternating marine and fluvial facies containing numerous unconfined and confined groundwater aquifers (Chen, 2008). The aquifer in the littoral plain is a sandy lens up to 20 m thickness, which constitutes the water source to the coastal residents and fishing ports (Liao et al., 2005; Chen, 2008).

2.2 Sampling and measurements

Our cruise, which was organized under the South China Sea Coastal Oceanographic Process Experiment (SCOPE), was carried out from 30 June to 8 July, 2008 (Leg 1) onboard the R/V *Shiyan III*. The cruise began from the PRE, and continued on to the east of Taiwan shoal in the NSCS, where water depths and distance offshore ranged from 25 to 350 m and 15 to 180 km, respectively (Fig. 1). Samples used for this study were collected along seven cross-shelf transects (designated as 1–7). Large volume samples (from 50 L near shore to 100 L offshore) for Ra isotopes were pumped from ~5 m below the surface by a submersible pump through a 1 µm cartridge filter and then into a polypropylene container. Subsurface seawater samples were taken by 30-L Niskin bottles mounted on a Rosette sampler equipped with a calibrated SBE-19-plus Conductivity-Temperature-Depth (CTD) recorder (Sea-Bird Co.) that measured water temperature and salinity. Detailed cruise information has been reported in Cao et al. (2011).

In addition to seawater collection from the cruise, we sampled coastal groundwater and spring water along the NSCS shelf in December 2008 (red inverted triangle in Fig. 1) and October 2010 (blue triangle in Fig. 1). Additional sampling information is provided in the Supplement.

After recording the sample volume, we passed the water through a column of MnO₂ coated acrylic fiber (Mn fiber) via gravity with a flow rate less than 1 L per minute to quantitatively remove Ra (Moore, 1976; Moore, 2007).

2.2.1 Measurements of short-lived and long-lived Ra isotopes

In the laboratory, we washed Mn fiber samples with Ra free deionized water to remove the sea salts, flushed with compressed air for ~7 min to adjust to an appropriate moisture content and then placed it in a Radium Delayed Coincidence Counter (RaDeCC) system to determine the short-lived radium isotopes, ²²³Ra ($T_{1/2}$ = 11.4 days) and ²²⁴Ra ($T_{1/2}$ = 3.7 days) (Moore and Arnold, 1996; Moore, 2008). This delayed coincidence system differentiates the alpha particle signals derived from ²¹⁹Rn and ²²⁰Rn, which are the decay daughters of ²²³Ra and ²²⁴Ra, respectively (Giffin et al., 1963; Moore and Arnold, 1996). The associated uncertainties of the measurements were estimated according to Garcia-Solsona et al. (2008).

After the measurements of ²²³Ra and ²²⁴Ra, we used two methods to determine long-lived Ra isotopes. One of the methods involved recounting the Mn fiber using the RaDeCC system in ~6 months after sample collection, which allowed for ingrowth of ²²⁸Th from its precursor, ²²⁸Ra ($T_{1/2}$ = 5.75 years). Upon correction for the decay of ²²⁸Th that was originally coated on the Mn fiber from the initial samples, we obtained the ²²⁸Ra activity as described in Moore et al. (2008). Our second approach to measure ²²⁶Ra and ²²⁸Ra was gamma counting. Except for the groundwater samples taken in 2010, our Mn fiber samples were leached with a mixture of 1 mol L⁻¹ hydroxylamine hydrochloride and hydrogen peroxide solution at 50 °C. Radium-228 and ²²⁶Ra ($T_{1/2}$ = 1600 years) in the solution were co-precipitated with BaSO₄ and the precipitate was sealed in a small counting vial for 3 weeks prior to the measurement with a well-type germanium detector (ORTEC, GWL-120-15-S). Radium-228 and ²²⁶Ra were determined from their daughters ²²⁸Ac (peaks at 911 keV) and ²¹⁴Pb (peaks at 295 and 352 keV), respectively (Moore, 1984; Moore et al., 1985; Chen et al., 2010). The

How significant is submarine groundwater discharge?

Q. Liu et al.

Title Page

Abstract

Introduction

Conclusions

References

Tables

Figures



Back

Close

Full Screen / Esc

Printer-friendly Version

Interactive Discussion

errors for the ^{228}Ra and ^{226}Ra measurements were in the range of 5-26% (1σ ; based on counting statistics and standard propagation of errors).

2.2.2 Measurements of major ions, carbonate system parameters, and inorganic nutrients

5 Samples for sodium, magnesium, and calcium analyses were filtered through a 0.45 μm membrane filter and refrigerated. They were then analyzed on a Dionex ICS-2500 ion chromatograph. The detailed description of sampling and measurement of inorganic carbon and nutrients in this cruise were presented in Cao et al. (2011) and Han et al. (2011), respectively. These chemical parameters in groundwater samples were
10 measured using the same methods as those for the estuary and shelf waters.

3 Results

3.1 Hydrography and hydrochemistry in the NSCS

The basic hydrological information during this cruise was reported in Shu et al (2011a, b) and Gan et al (2009a, b). In brief, there was continuous rainfall ten days prior to our
15 cruise in the drainage basin of the Pearl River, resulting in nearly doubled water discharge as compared to the long term average in the wet season (Cao et al., 2011). The abundant river discharge clearly resulted in a large plume of water that spreading eastward over the shelf as seen from the salinity distribution (Fig. 2b). A minimum salinity of 26.6 was measured at the site S106 about 70 km away from the PRE. This plume water
20 also appeared at ~ 350 km towards the Taiwan Shoal over the NSCS shelf, with warm temperatures (27.2–30.2 $^{\circ}\text{C}$) and low salinities (26.6–33.3) (Fig. 2b), indicating eastward spreading driven by the southeast monsoon. We observed that the shelf regions laced with these plume waters were characterized by low DIC (Cao et al., 2011) but high inorganic nitrogen ($\text{NO}_3^- + \text{NO}_2^-$) and relatively low PO_4 and Si (Han et al., 2011),

How significant is submarine groundwater discharge?

Q. Liu et al.

Title Page

Abstract

Introduction

Conclusions

References

Tables

Figures



Back

Close

Full Screen / Esc

Printer-friendly Version

Interactive Discussion



indicating that DIC was reduced by the enhanced biological consumption caused by the high nutrients supplied from the Pearl River plume.

In addition to the plume, the study area is characterized by coastal upwelling as demonstrated by the relatively high salinity (averaging 33.8) and low temperature (averaging 23.7°C) at the inner shelf stations from transects 4 to 7 (Fig. 2a and b) (Gan et al., 2010; Shu et al., 2011a). Not surprisingly, the upwelled water was enriched in DIC, TA, and TAlk (Cao et al., 2011), and nutrients (Han et al., 2011). Note that the apparent distribution pattern of nutrients and carbonate is a result of the co-influence of the upwelled water mixed with nearshore surface water and biological productivity, because the Pearl River plume and the coastal upwelling are spatially interactive. The plume is transported by the upwelling circulation, while the buoyancy of the plume modulates the upwelling circulation over the shelf. The cross section of temperature and salinity along transect 2 demonstrated that the bottom cold water (19.2–21.3°C) encroached onto the shelf from the slope at ~100 m but it did not outcrop at the surface due to the stratification induced by the low salinity (25.7–33.3) Pearl River plume (Fig. 3).

3.2 Ra distributions on the NSCS shelf

3.2.1 Surface distributions of Ra isotopes on the NSCS shelf

Surface Ra activity showed considerable spatial variations in the study area (Fig. 2c to f, and Table 1). Radium-228, ^{226}Ra , ^{223}Ra , and excess ^{224}Ra ranged from 6.85 to 61.2, 5.15 to 27.9, 0.02 to 1.94, and 0.09 to 44.0 dpm 100 L⁻¹, respectively. One unique feature of ^{228}Ra distribution in the NSCS compared with other shelf areas (e.g. Moore, 2000b) was an increase in activity with distance offshore. This can be attributed to eastward dispersal of the high-radium river plume offshore relative to the coastal upwelling nearshore. Figure 2e showed relatively low ^{228}Ra activity on the inner shelf (longitude and latitude ranged from 116.7 to 117.7° E, from 22.9 to 23.5° N) in the range of 12.4 to 29.2 dpm 100 L⁻¹, which is mainly controlled by coastal upwelling, suggesting that bottom/subsurface water with low ^{228}Ra activity outcropped to the surface. In contrast,

BGD

8, 12381–12422, 2011

How significant is submarine groundwater discharge?

Q. Liu et al.

Title Page

Abstract

Introduction

Conclusions

References

Tables

Figures

◀

▶

◀

▶

Back

Close

Full Screen / Esc

Printer-friendly Version

Interactive Discussion



there were higher ^{228}Ra activities in the Pearl River plume zone, which matched well with the salinity pattern (Fig. 2b). The highest ^{228}Ra ($61.2 \text{ dpm } 100 \text{ L}^{-1}$) appeared at the station closest to the PRE (S106), corresponding to the low salinity center of the plume (Fig. 2b). Radium-226 in the surface water of the NSCS followed the same pattern (Fig. 2f), suggesting its distribution is controlled by the same source and transport processes.

The distribution of $\text{ex } ^{224}\text{Ra}$ (excess ^{224}Ra , corrected for the ingrowth from ^{228}Th) (Fig. 2d) was significantly different from those of long-lived Ra isotopes (^{226}Ra and ^{228}Ra). The presence of the highest $\text{ex } ^{224}\text{Ra}$ in the coastal upwelling region suggests a potential subsurface source for this isotope. In contrast, measurable Pearl River plume $\text{ex } ^{224}\text{Ra}$ was not apparent (except at S106), likely because the half-life of ^{224}Ra ($T_{1/2} = 3.7$ days) is too short to trace the Pearl River plume farther off the estuary. Radium-223 (Fig. 2c) was relatively high in the Pearl River plume, ranging from 0.72 to $1.91 \text{ dpm } 100 \text{ L}^{-1}$, a likely result of its longer half life ($T_{1/2} = 11.4$ days). Like $\text{ex } ^{224}\text{Ra}$, high ^{223}Ra (0.72 to $1.51 \text{ dpm } 100 \text{ L}^{-1}$) existed in the nearshore coastal upwelling zone (Fig. 2c). However, it was hard to differentiate the ^{223}Ra from the river plume and from coastal upwelling since the ^{223}Ra activity was similar in these two zones (Fig. 2c).

3.2.2 Vertical distributions of Ra isotopes on the NSCS shelf

To verify the impact of subsurface/bottom water on the distributions of Ra isotopes in surface waters, we sampled the water column at stations S201, S702 and S305 (Fig. 1). Figure 4a shows ^{226}Ra and ^{228}Ra activities at site S201 decreased with depth while $\text{ex } ^{224}\text{Ra}$ and ^{223}Ra activities increased with depth. These distributions provide strong evidence that upwelling would elevate $\text{ex } ^{224}\text{Ra}$ and ^{223}Ra but lower ^{228}Ra and ^{226}Ra activities in surface waters.

To further provide a composite view of which isotopes tracked what individual processes, we plotted temperature and salinity with the data of various Ra isotopes superimposed on the plot (Fig. 5). Again, short-lived Ra isotopes ($\text{ex } ^{224}\text{Ra}$ and ^{223}Ra)

BGD

8, 12381–12422, 2011

**How significant is
submarine
groundwater
discharge?**

Q. Liu et al.

Title Page

Abstract

Introduction

Conclusions

References

Tables

Figures

⏪

⏩

◀

▶

Back

Close

Full Screen / Esc

Printer-friendly Version

Interactive Discussion



were enhanced in both the subsurface water and river plume, but were reduced in the surface seawater. In contrast, long-lived Ra isotopes (^{228}Ra and ^{226}Ra) were enriched in the river plume area, but were low in both the surface SCS seawater and subsurface water/upwelling zone. Thus, Ra isotopes will be applied to assess the transport rate of the Pearl River plume and the coastal upwelling during our sampling period (See Sect. 4.1).

3.3 Surface distributions of Ra isotopes in the Pearl River estuary

The radium versus salinity plots (Fig. 6) revealed that all of the four Ra isotopes were distributed coherently in surface waters of the PRE, i.e. with low activities at zero salinity, followed by an increase with salinity until reaching the highest activities at salinities of 2.5–10. Ra activities decreased then toward the lowest values in high salinity seawater. Such a pattern has been observed in estuaries of other large rivers, such as the Chao Phraya River and the Mississippi River and may reflect release of Ra isotopes from particles into solution upon estuarine mixing (Krest et al., 1999; Moore and Krest, 2004; Dulaiova and Burnett, 2006).

3.4 Ra isotopes and other dissolved constituents in the NSCS groundwater

We sampled freshwater supply-wells (salinity near nil) and one saline spring (salinity was 7.2) along the shoreline in 2008 (Table S1 in the Supplement). In 2010, we collected both fresh (salinity: 0–0.5) and brackish groundwater (salinity: 8.5–24.3) as pore water within the beach sediments along the NSCS shelf (Table S1 in the Supplement). Briefly, Ra activities were enriched in all of the groundwater samples with an average of $25.0 \pm 1.45 \text{ dpm } 100 \text{ L}^{-1}$ for ^{223}Ra , $686 \pm 7.12 \text{ dpm } 100 \text{ L}^{-1}$ for ^{224}Ra , $124 \pm 8.45 \text{ dpm } 100 \text{ L}^{-1}$ for ^{226}Ra , and $413 \pm 10.2 \text{ dpm } 100 \text{ L}^{-1}$ for ^{228}Ra , all of which were higher relative to those in the river plume (average of $0.93 \pm 0.02 \text{ dpm } 100 \text{ L}^{-1}$, $6.25 \pm 0.09 \text{ dpm } 100 \text{ L}^{-1}$, $18.2 \pm 0.81 \text{ dpm } 100 \text{ L}^{-1}$, and $41.6 \pm 0.10 \text{ dpm } 100 \text{ L}^{-1}$, respectively) and offshore ($0.07 \pm 0.02 \text{ dpm } 100 \text{ L}^{-1}$,

BGD

8, 12381–12422, 2011

How significant is submarine groundwater discharge?

Q. Liu et al.

Title Page

Abstract

Introduction

Conclusions

References

Tables

Figures

⏪

⏩

◀

▶

Back

Close

Full Screen / Esc

Printer-friendly Version

Interactive Discussion



2.62 ± 0.15 dpm 100 L⁻¹, 5.15 ± 0.80 dpm 100 L⁻¹, and 7.10 ± 0.91 dpm 100 L⁻¹, respectively). Similarly, groundwater has high concentrations of nutrients, DIC, and TALK compared with surface waters. Silicate displayed conservative mixing between a high groundwater end-member and much lower values in seawater. In contrast, NH₄⁺, PO₄³⁻, DIC, and TALK showed increases while NO₃⁻ + NO₂⁻ showed decreases during the mixing of fresh groundwater with seawater in the coastal aquifer, likely due to denitrification or other organic degradation processes (Slomp and Van Cappellen, 2004). Detailed descriptions of the concentrations of the solutes and their variabilities can be found in the Supplement.

4 Discussions

4.1 Water ages derived from ²²³Ra/²²⁸Ra

Water age is a key variable in understanding chemical and biological processes of riverine plumes and nearshore upwelling and also necessary to determine the fluxes of SGD and associated terrestrial materials. This can be estimated via physical methods (Pilson, 1985; Sanford et al., 1992), numerical models (Das et al., 2000), or isotopic water mass balances (Kelly and Moran, 2002; Delhez et al., 2003; Rasmussen, 2003). Ra isotopes have been used to estimate the time elapsed since a water parcel was last in contact with a boundary (Charette et al., 2008). Here, we used ²²³Ra/²²⁸Ra activity ratio to estimate the water age. The normalization to the long-lived ²²⁸Ra was to eliminate the effect of mixing processes. The mathematical equation can be represented as (Moore, 2000a; Charette et al., 2001):

$$\left[\frac{\text{ex}^{223}\text{Ra}}{\text{ex}^{228}\text{Ra}} \right]_{\text{obs}} = \left[\frac{\text{ex}^{223}\text{Ra}}{\text{ex}^{228}\text{Ra}} \right]_i e^{-\lambda_{223}\tau} \quad (1)$$

where, ex represents the measured Ra concentration in excess of the value in the offshore surface water (0.07 dpm 100 L⁻¹ for ²²³Ra, 7.10 dpm 100 L⁻¹ for ²²⁸Ra).

How significant is submarine groundwater discharge?

Q. Liu et al.

Title Page

Abstract

Introduction

Conclusions

References

Tables

Figures

◀

▶

◀

▶

Back

Close

Full Screen / Esc

Printer-friendly Version

Interactive Discussion



average water age on the NSCS shelf is in very good agreement with the physical modeling estimation (13.5 days) with the currents driven by idealized constant wind stress (Jianping Gan, Hong Kong University of Science and Technology, personal communication).

4.2 Submarine groundwater discharge

Shown in Fig. 6 are the plots of radium distribution against salinity, which can be used to further examine various Ra sources. There were distinguishable Ra additions with regard to the conservative mixing line between the river and seawater end-members (solid line in Fig. 6). In the PRE, these additions could be explained by ion exchange with suspended fluvial particles, diffusion from sediments, and SGD. After salinity driven desorption has run its course within the estuary, Ra should behave conservatively. Thus, unlike that in the estuary, there was no Ra peak at intermediate salinity on the NSCS shelf. The radium/salinity relationships also reveal Ra sources other than Pearl River plume and seawater mixing on the NSCS shelf (Fig. 6). Elevated ^{224}Ra and ^{223}Ra were present at high salinity (33.3–34.0) where the influence of coastal upwelling was strong. Excluding the upwelling zone, excess ^{223}Ra can be contributed by SGD and diffusion from sediments, which was not apparent with ^{224}Ra in the shelf water because of decay during mixing. Alternatively, we believe that long-lived Ra isotopes could be unambiguous tracers of SGD in the NSCS mainly due to their long half-lives and less diffusion from sediments. Firstly, Ra was enriched in groundwater compared with river plume and seawater. Secondly, Ra behaved conservatively after entering the marine water. Therefore, we used two independent methods involving the long-lived Ra isotopes to estimate SGD flux, discussed as follows.

BGD

8, 12381–12422, 2011

How significant is submarine groundwater discharge?

Q. Liu et al.

Title Page

Abstract

Introduction

Conclusions

References

Tables

Figures

⏪

⏩

◀

▶

Back

Close

Full Screen / Esc

Printer-friendly Version

Interactive Discussion

4.2.1 SGD flux derived from a three end-member mixing model on the NSCS shelf

We identified three potential end-members contributing to radium isotopes in the NSCS surface water: the Pearl River plume, SGD, and the surface SCS water. Here, we excluded the upwelling zone because there is no pronounced difference of $^{226/228}\text{Ra}$ between upwelling water and SCS surface seawater and we did not collect offshore subsurface water, which would otherwise allow us to define the end-member concentration (Fig. 5c and d). By definition SGD includes meteoric water from land drainage and seawater that exchanges with the coastal aquifer (Burnett et al., 2003). Since the composition of these two SGD components was unknown and we had a limited number of groundwater samples, it was difficult to determine the average salinity of the SGD end-member.

During our cruise, no significant biogenic CaCO_3 production or dissolution occurred (Cao et al., 2011) and TALK behaved conservatively. We found low TALK in the Pearl River plume and high values in the subsurface waters (Fig. 5e). Based on these end-member concentrations, TALK and $^{226/228}\text{Ra}$ were used to estimate the SGD to the NSCS shelf. Additionally, the relationship between ^{228}Ra and TALK (Fig. 7) clearly indicated a third source to the shelf that we inferred to be SGD. To this end, the following equations were used to establish the three end-member model,

$$f_S + f_P + f_{\text{GW}} = 1 \quad (3)$$

$${}^i\text{Ra}_S f_S + {}^i\text{Ra}_P f_P + {}^i\text{Ra}_{\text{GW}} f_{\text{GW}} = {}^i\text{Ra}_M \quad (4)$$

$$\text{Alk}_S f_S + \text{Alk}_P f_P + \text{Alk}_{\text{GW}} f_{\text{GW}} = \text{Alk}_M \quad (5)$$

where the subscripts S, P, and GW refer to the oceanic, Pearl River plume, and surficial groundwater end-members, respectively. The subscript M represents the measured values for individual samples, the parameter f is fraction of water derived from various end-members, the superscript i is 226 or 228, Ra is Ra isotope activity ($\text{dpm } 100 \text{ L}^{-1}$)

BGD

8, 12381–12422, 2011

How significant is submarine groundwater discharge?

Q. Liu et al.

Title Page

Abstract

Introduction

Conclusions

References

Tables

Figures

⏪

⏩

◀

▶

Back

Close

Full Screen / Esc

Printer-friendly Version

Interactive Discussion



and Alk is total alkalinity (mmol m^{-3}). Radium-226 and ^{228}Ra decay is negligible on the time scale of mixing processes in the study region. In this three end-member mixing model, the largest uncertainty is the groundwater end-member of Ra, because we lack brackish groundwater Ra samples in 2008. The ^{228}Ra activity in groundwater collected in 2008 and 2010 ranged from 30.2–872 dpm 100 L^{-1} (Table S1 in the Supplement), and here we averaged all of the high ^{228}Ra ($>400\text{ dpm } 100\text{ L}^{-1}$) samples in 2008 and 2010 as the groundwater end-member. Note that such groundwater end-members would imply an underestimation of SGD because the higher Ra end-member in groundwater would make the SGD rate lower (See Sect. 4.2.3). For ^{226}Ra , the average of $124 \pm 10.6\text{ dpm } 100\text{ L}^{-1}$ in 2008 was used as the groundwater end-member since we did not measure ^{226}Ra for groundwater in 2010. For the TALK end-member in groundwater, we took the average from all groundwater (4020 mmol m^{-3}) sampled in 2008 and 2010 as the end-member value. The ^{226}Ra end-member values for the offshore surface water and river plume were 5.15 ± 0.80 and $20.7 \pm 0.90\text{ dpm } 100\text{ L}^{-1}$, respectively. The ^{228}Ra end-member values for the offshore surface water and river plume were 7.10 ± 0.92 and $62.3 \pm 1.01\text{ dpm } 100\text{ L}^{-1}$, respectively. The TALK end-member values in the offshore surface water and river plume were 2272 and 1966 mmol m^{-3} , respectively.

The model results are shown in Figs. 7 and 8. The groundwater fraction in the NSCS (f_{GW}) was in the range of 0 to 5% (mean $1.5 \pm 1.6\%$) based on the $^{228}\text{Ra}/\text{TALK}$ relationship and 0–9.7% (mean $2.5 \pm 2.6\%$) using the $^{226}\text{Ra}/\text{TALK}$ relationship. The Pearl River plume contribution to shelf waters ranged from 0.1–83% with an average of 38%.

We also calculated the volumetric SGD rate ($\text{m}^3\text{ d}^{-1}$) on the NSCS shelf using the formula:

$$\text{SGD} = f_{\text{GW}} \times V_{\text{SW}} / \tau \quad (6)$$

where V_{SW} is the water volume above the mixed layer in the study region (m^3) and τ is the radium-derived water age (days). We used 245 km^3 for V_{SW} and 16.3 ± 10.3 days

How significant is submarine groundwater discharge?

Q. Liu et al.

[Title Page](#)[Abstract](#)[Introduction](#)[Conclusions](#)[References](#)[Tables](#)[Figures](#)[⏪](#)[⏩](#)[◀](#)[▶](#)[Back](#)[Close](#)[Full Screen / Esc](#)[Printer-friendly Version](#)[Interactive Discussion](#)

for τ , as derived from the $^{223}\text{Ra}/^{228}\text{Ra}$ AR age model. By solving Eq. (6), the SGD flux from the ^{228}Ra -TALK and ^{226}Ra -TALK mixing models was $2.3 \pm 2.8 \times 10^8$ and $3.7 \pm 4.6 \times 10^8 \text{ m}^3 \text{ d}^{-1}$, respectively.

4.2.2 Radium mass balance approach for estimating SGD

Our second approach to quantify the SGD fluxes is based on Ra mass balance, which has been frequently used (Charette et al., 2008 and reference therein), as illustrated in Fig. 9. Under steady state, Ra inventory is balanced by all the Ra inputs, which can be expressed as follows:

$$\frac{\text{Inventory}^i \text{Ra}}{\tau} = [F_{\text{Riv}} \times {}^i \text{Ra}_{\text{Riv}}] + [A_{\text{Sed}} \times \text{Ra}_{\text{Sed}}] + [\text{SGD} \times {}^i \text{Ra}_{\text{Gw}}] + [\nu \times {}^i \text{Ra}_{\text{Uw}} \times A_{\text{Uw}}] \quad (7)$$

where, the left term is the total Ra input flux, and the right terms represent various Ra sources including the contributions from dissolved Ra and release from suspended particles in the Pearl River, diffusive benthic input, SGD flux, and coastal upwelling input. Since SGD is the only unknown in Eq. (7), it can be calculated. In order to compare the SGD flux evaluated from the three end-member mixing model with the result derived from this box model without the upwelling zone, we performed two iterations of this box model: with and without upwelling. Summarized in Table 3 are the definitions, values and units of the terms involved in the box model.

The discharge rate of the Pearl River was the sum of the average rates of the three tributaries one week prior to the sampling. For the SGD calculation, we only estimated the groundwater input along the coastline but excluded the SGD from PRE. The maximum ^{226}Ra and ^{228}Ra in the PRE were used as inputs from the river, including dissolved and suspended particles released Ra. Two surface sediments taken near S201 are mainly composed of different sizes of sands and small amount of silts, which was agreeable with sediment type reports for the NSCS (Hiroshi and Emery, 1961; Luo et al., 1985; Zhang et al., 2003). We did not perform sediment incubation experiments to directly measure the diffusive Ra flux, but instead took the average from globally

How significant is submarine groundwater discharge?

Q. Liu et al.

Title Page

Abstract

Introduction

Conclusions

References

Tables

Figures



Back

Close

Full Screen / Esc

Printer-friendly Version

Interactive Discussion



How significant is submarine groundwater discharge?

Q. Liu et al.

Title Page

Abstract

Introduction

Conclusions

References

Tables

Figures

⏪

⏩

◀

▶

Back

Close

Full Screen / Esc

Printer-friendly Version

Interactive Discussion

available regeneration rate of 0.45 and $25 \text{ dpm m}^{-2} \text{ d}^{-1}$ for ^{226}Ra and ^{228}Ra (Krest et al., 1999; Hancock et al., 2000; Charette et al., 2001; Hancock et al., 2006), respectively. The reported average activities for ^{226}Ra , ^{228}Ra , and ^{228}Th in NSCS surface sediments was 1.66 ± 0.08 , 2.70 ± 0.35 , $2.52 \pm 0.36 \text{ dpm g}^{-1}$, respectively (Liu et al., 2001). As these activities are typical of the other studies cited above, we are confident that the potential diffusive Ra flux is small. We calculated the upwelling water volume by multiplying the surface of the area zone with the water depth. The average ^{228}Ra ($27.9 \pm 2.72 \text{ dpm } 100 \text{ L}^{-1}$) and ^{226}Ra ($8.26 \pm 0.78 \text{ dpm } 100 \text{ L}^{-1}$) in three bottom waters (S201-15, S305-60, and S702-15) were used as the Ra end-member for the upwelled water.

In our Ra inventory estimation, we did not take into account the whole water column but only used a single surface sample to represent the whole mixed layer because not enough bottom samples were collected. Excess Ra was the measured activity on the NSCS shelf subtracted from the values in the offshore surface water ($5.15 \pm 0.80 \text{ dpm } 100 \text{ L}^{-1}$ for ^{226}Ra , $7.10 \pm 0.91 \text{ dpm } 100 \text{ L}^{-1}$ for ^{228}Ra). Following the method used by Moore (2007) for the southeastern U.S. continental shelf, we derived total excess Ra inventory on the NSCS shelf.

Table 4 summarizes all sources that contributed to the total ^{226}Ra and ^{228}Ra flux into the NSCS, among which, dissolved Ra and suspended particles released from Pearl River comprised 26–50 % of the total Ra flux, which was comparable to the SGD contribution of 38–48 %. Unlike in non river-dominated marginal systems, Ra input from SGD dominated the total Ra flux in the coastal ocean.

Our estimated SGD rate without upwelling was 2.8×10^8 and $3.9 \times 10^8 \text{ m}^3 \text{ d}^{-1}$ based on the ^{228}Ra and ^{226}Ra mass balance, respectively. The calculated groundwater input including the nearshore upwelling zone was slightly higher than that without upwelling, with averaged SGD of 3.3×10^8 and $4.5 \times 10^8 \text{ m}^3 \text{ d}^{-1}$ from ^{228}Ra and ^{226}Ra , respectively.

4.2.3 Comparison of the two methods for estimating SGD

Comparing these two approaches, we obtained average SGD fluxes of $3.1 \pm 2.7 \times 10^8 \text{ m}^3 \text{ d}^{-1}$ and $3.3 \pm 3.4 \times 10^8 \text{ m}^3 \text{ d}^{-1}$ (excluding the nearshore upwelling zone) via the Ra-TALK three end-member mixing model and Ra mass balance model, respectively. The good agreement between these two independent approaches gives us confidence that our estimated SGD fluxes are well grounded. The SGD fluxes for the 308 km NSCS coastline ranged from $3.3\text{--}4.5 \times 10^8 \text{ m}^3 \text{ d}^{-1}$ when including the upwelling zone (Table 2). When scaled to the coastline length, the SGD rate was $1100\text{--}1461 \text{ m}^3 \text{ m}^{-1} \text{ d}^{-1}$, comparable to some other regional-scale studies, such as the South Atlantic Bight ($5.5\text{--}6.2 \times 10^8 \text{ m}^3 \text{ d}^{-1}$; Moore, 2010b) and Sicily/Mediterranean ($1000 \text{ m}^3 \text{ m}^{-1} \text{ d}^{-1}$; Moore, 2006).

The three end-member mixing model is very sensitive to the end-member of plume and seawater values: a 5% variation in TALK can change the SGD flux by 59.5–75.2% (Table 2). Fortunately, the TALK of these two end-members was relatively constant with only 0.95–1.75% variation on our cruise (Cao et al., 2011). The most variable end-members were TALK and Ra in coastal groundwater; fortunately, the model is much less sensitive to changes in this term (6.0–7.5% SGD change with 5% end-member variation). The higher the TALK/Ra end-member for groundwater, the lower the SGD flux will be obtained. TALK in groundwater had a large spatial variation, ranging from 381 to 9009 $\mu\text{mol L}^{-1}$ (Table S1 in Supplement). However, the SGD rate would change 61% with the usage of the maximum TALK compared with the average, a change that is within the bounds of the error estimation of the model. Notably, the re-estimated SGD would not change within uncertainties even if the groundwater Ra end-member was increased by 300%.

Uncertainty analysis exhibited that the Ra mass balance is highly sensitive to the water age (Table 2). A variation of 1 day would cause a change of 21–26% in the SGD rate. It should be noted that the average water age in our study area has a standard deviation of ~ 10 days, which could produce one order of magnitude change in SGD

BGD

8, 12381–12422, 2011

How significant is submarine groundwater discharge?

Q. Liu et al.

Title Page

Abstract

Introduction

Conclusions

References

Tables

Figures

⏪

⏩

◀

▶

Back

Close

Full Screen / Esc

Printer-friendly Version

Interactive Discussion



fluxes. However, much of this variability is likely natural, as water age is expected to vary with distance from the coastline; given the scale of our model domain we do not feel that this is a major source of uncertainty in our SGD estimates. The uncertainty from the sediment diffusion was small for ^{226}Ra mass balance due to its long half-life, but might be significant for the ^{228}Ra model. As presented in Table 4, the ^{228}Ra flux from benthic sediment diffusion contributed 16 % and 25 % of total ^{228}Ra flux in our model without and with upwelling, respectively. It contributed 25 % of the uncertainty in our model. Given that these estimates were obtained from the literature and applied to our study, the ^{226}Ra balance model should be considered to be more reliable than the ^{228}Ra model in this regard. Though our upwelling-derived Ra flux was not well constrained, our Ra box model was not sensitive to this Ra source. In addition, the bottom Ra activity decreased offshore from three bottom samples in this cruise and the same phenomenon was observed during other seasons on the NSCS shelf (Dai, unpublished data), therefore, our selection of the Ra end-member in the upwelled water would result in a conservative, lower limit estimation of SGD. Like the three end-member mixing model, the uncertainty from the Ra activity in groundwater was small (4.8 % SGD change with 5 % end-member variation). Other error sources, such as Ra end-member in offshore and in the estuary, are relatively easy to determine.

In general, Ra is usually enriched in brackish groundwater relative to fresh groundwater (Mulligan and Charette, 2006) due to cation exchange processes (Li et al., 1977). For example, ^{228}Ra concentrations increase 100-fold when fresh groundwater mixes with seawater in the subterranean estuary (Moore et al., 2008). However, in some cases, high Ra activities in fresh groundwater also have been reported (Moore, 2003; Charette and Buesseler, 2004). High ^{228}Ra activity existed in fresh groundwater in 2008, concurrently with our cruise, and brackish groundwater in 2010. Even though we did not collect high salinity groundwater samples in 2008, we presume that ^{228}Ra in brackish groundwater in 2008 was close or higher than fresh groundwater in 2008. The average net annual groundwater recharge rate was $1\text{--}1.8 \times 10^7 \text{ m}^3 \text{ d}^{-1}$ into the groundwater system along the shoreline of our study site from 1956 to 2000 (Liao et

How significant is submarine groundwater discharge?

Q. Liu et al.

[Title Page](#)[Abstract](#)[Introduction](#)[Conclusions](#)[References](#)[Tables](#)[Figures](#)[Back](#)[Close](#)[Full Screen / Esc](#)[Printer-friendly Version](#)[Interactive Discussion](#)

al., 2005; Chen, 2008), which is only 4–9% of our estimated SGD. Our data therefore support the idea that most of the SGD came from recirculated seawater.

4.3 SGD-induced nutrient and DIC fluxes on the NSCS shelf

Given the Ra-derived SGD rate and non-conservative nutrient behavior during SGD-driven seawater recirculation (i.e., concentration difference between saline groundwater and seawater), we estimated nutrient inputs to the NSCS from SGD of $9\text{--}18 \times 10^9 \text{ mol yr}^{-1}$ for NO_3^- and $15\text{--}30 \times 10^7 \text{ mol yr}^{-1}$ for PO_4^{3-} ; these were equivalent to 49–96%, 50–99% of the inputs of the Pearl River for NO_3^- and PO_4^{3-} , respectively, in the wet season (Cai et al., 2004). With respect to SiO_4^{4-} discharge, which displayed conservative behavior in groundwater, we utilized the product of fresh SGD and SiO_4^{4-} in the fresh groundwater end-member to derive an export flux of $1\text{--}2 \times 10^9 \text{ mol yr}^{-1}$ to the NSCS shelf, which was equivalent to 3–6% of the riverine SiO_4^{4-} input in the wet season (Cai et al., 2004).

Using the same approach for the carbonate system, we obtained a SGD contribution of $266\text{--}520 \times 10^9 \text{ mol yr}^{-1}$ DIC and $245\text{--}479 \times 10^9 \text{ mol yr}^{-1}$ TAlk to the NSCS shelf, which represented 44–73% and 40–68% of the riverine DIC and TAlk fluxes in the wet season (Guo et al., 2008). The SGD-associated DIC flux was $\sim 10\text{--}19\%$ of coastal upwelling-derived DIC (DIC end-member in subsurface water was presented in Cao et al., 2011). For other sites where groundwater-surface water DIC fluxes have been quantified, our estimate is similar to those for salt marshes in Georgia and South Carolina (Cai et al., 2003), but higher than that in the Okatee estuary (Moore et al., 2006) and Williams Lake and Shingobee Lake in Minnesota (Striegl and Michmerhuizen, 1998).

Once released to surface water, SGD-derived DIC could be consumed by biological production stimulated by the nutrients loaded from groundwater. The net effect on the inorganic carbon budget in the coastal ocean from SGD will therefore be modulated by the balance of these two processes. In the Pearl River plume over the NSCS shelf was

BGD

8, 12381–12422, 2011

**How significant is
submarine
groundwater
discharge?**

Q. Liu et al.

Title Page

Abstract

Introduction

Conclusions

References

Tables

Figures

⏪

⏩

◀

▶

Back

Close

Full Screen / Esc

Printer-friendly Version

Interactive Discussion



characterized by P limitation (Han et al., 2011). Using Redfield Ratios, SGD-derived P may be responsible for new production up to 3–6 mmol C m⁻² d⁻¹. This rate of new production would at most reduce the DIC flux by 35–68 × 10⁹ mol C yr⁻¹, which is 18 % of the SGD-driven DIC rate. If we assume that the water volume of the mixed layer is 311 km³ and the average water age is 14.3 days, then SGD inputs could support DIC and TAlk increases of 29–57 μmol L⁻¹ and 32–60 μmol L⁻¹ on the NSCS shelf, respectively. Since water column DIC concentrations could also be affected by gas exchange, these values represent the upper limit. Nevertheless, we conclude that SGD in our system is a net source of DIC and TAlk and likely plays a significant role in the carbonate system over the NSCS shelf.

5 Conclusions

This study demonstrated that submarine groundwater discharge (SGD) can be a significant source of inorganic carbon to a RioMar shelf subject to abundant freshwater input from large rivers. The complex hydrogeologic regime in these systems requires multiple tracers in order to differentiate the multiple source terms including surface and groundwater inputs as well as subsurface water via upwelling. To this end, our study highlights the feasibility of using radium isotopes combined with TAlk to estimate SGD fluxes. The independent approaches we adopted based on three end-member mixing and mass balance have revealed consistent results, which were 2.3–3.7 × 10⁸ m³ d⁻¹ and 2.8–4.5 × 10⁸ m³ d⁻¹, respectively. These fluxes were equivalent to ~19% of the Pearl River discharge in wet season.

We estimate that DIC flux carried by the groundwater discharge represented ~59% and ~15% of the DIC contributions from the river plume and coastal upwelling, respectively. To our knowledge, this is the first evaluation of SGD flux and its impact on the budget of coastal inorganic carbon in a river-dominated marginal system. Such DIC export from the groundwater may have significant impact on the carbonate system over the shelf. We also note that, since SGD also carries nutrients, the net effect of

BGD

8, 12381–12422, 2011

How significant is submarine groundwater discharge?

Q. Liu et al.

Title Page

Abstract

Introduction

Conclusions

References

Tables

Figures

⏪

⏩

◀

▶

Back

Close

Full Screen / Esc

Printer-friendly Version

Interactive Discussion



this DIC flux on the seawater DIC balance may be reduced. The interplay between the DIC and nutrient discharges will therefore depend on the hydrogeologic setting and the groundwater sources as well as the biogeochemical reactions taking place in the subsurface. Constraint of such end-members and their biogeochemical reactivity within coastal aquifers remains a big challenge in the field of SGD. Despite these uncertainties, however, we contend that SGD-associated carbon dioxide fluxes cannot be neglected in future regional and global carbon budgets.

Supplementary material related to this article is available online at:
<http://www.biogeosciences-discuss.net/8/12381/2011/bgd-8-12381-2011-supplement.pdf>.

Acknowledgements. This work was financially supported by the National Basic Research Program of China (973 Program) through grant #2009CB421204, and by the Natural Science Foundation of China (NSFC) through grants #90711005 and #40821063. Matthew Charette's participation was supported by a grant from the U.S. National Science Foundation (#OCE-0751525). The sampling cruise was supported by the SCOPE project co-organized by Jiang Zhu, Dongxiao Wang, Xiaogang Guo, Minhan Dai and Jianping Gan. We are grateful to Qian Li, Minquan Guo, Yang Liu, Wenbin Zhou, Nan Zheng, Jianrong Lin, Yuancheng Su, Xiao Huang, Lifang Wang, Hua Lin, and Zhangyong Wang for their help with ancillary data and sample collection. We also thank the crew of *Shiyan III* for their assistance at sea.

References

- Bokuniewicz, H., Taniguchi, M., Ishitoibi, T., Charette, M., Allen, M., and Kontar, E. A.: Direct measurements of submarine groundwater discharge (SGD) over a fractured rock aquifer in Flamengo Bay Brazil, *Estuar. Coast. Shelf S.*, 76, 466–472, 2008.
- Burnett, W. C., Bokuniewicz, H., Huettel, M., Moore, W. S., and Taniguchi, M.: Groundwater and pore water inputs to the coastal zone, *Biogeochemistry*, 66, 3–33, 2003.
- Burnett, W. C., Chanyotha, S., Wattayakorn, G., Taniguchi, M., Umezawa, Y., and Ishitobi, T.:

BGD

8, 12381–12422, 2011

How significant is submarine groundwater discharge?

Q. Liu et al.

Title Page

Abstract

Introduction

Conclusions

References

Tables

Figures

⏪

⏩

◀

▶

Back

Close

Full Screen / Esc

Printer-friendly Version

Interactive Discussion



How significant is submarine groundwater discharge?

Q. Liu et al.

Title Page

Abstract

Introduction

Conclusions

References

Tables

Figures

⏪

⏩

◀

▶

Back

Close

Full Screen / Esc

Printer-friendly Version

Interactive Discussion



Underground sources of nutrient contamination to surface waters in Bangkok, Thailand, *Sci. Total. Environ.*, 407, 3198–3207, 2009.

Cable, J. E., Burnett, W. C., Chanton, J. P., and Weatherly, G. L.: Estimating groundwater discharge into the northeastern Gulf of Mexico using radon-222, *Earth Planet. Sci. Lett.*, 144, 591–604, 1996.

Cai, W.-J., Wang, Y.-C., Krest, J., and Moore, W. S.: The geochemistry of dissolved inorganic carbon in a surficial groundwater aquifer in North Inlet, South Carolina, and the carbon fluxes to the coastal ocean, *Geochim. Cosmochim. Ac.*, 67, 631–639, 2003.

Cai, W.-J., Dai, M. H., Wang, Y. C., Zhai, W. D., Huang, T., Chen, S. T., Zhang, F., Chen, Z. Z., Wang, Z. H.: The biogeochemistry of inorganic carbon and nutrients in the Pearl River estuary and the adjacent Northern South China Sea, *Cont. Shelf Res.*, 24, 1301–1319, 2004.

Cao, Z., Dai, M., Zheng, N., Wang, D., Li, Q., Meng, F., and Gan, J.: Dynamics of the carbonate system in a large continental shelf system under the influence of both a river plume and coastal upwelling, *J. Geophys. Res.*, 116, G02010, doi:02010.01029/02010JG001596, 2011.

Capone, D. G. and Bautista, M.: A groundwater source of nitrate in nearshore marine sediments, *Nature*, 313, 214–216, 1985.

Charette, M. A.: Hydrologic forcing of submarine groundwater discharge: Insight from a seasonal study of radium isotopes in a groundwater-dominated salt marsh estuary, *Limnol. Oceanogr.*, 52, 230–239, 2007.

Charette, M. A. and Buesseler, K. O.: Submarine groundwater discharge of nutrients and copper to an urban subestuary of Chesapeake Bay (Elizabeth River), *Limnol. Oceanogr.*, 49, 376–385, 2004.

Charette, M. A., Buesseler, K. O., and Andrews, J. E.: Utility of radium isotopes for evaluating the input and transport of groundwater-derived nitrogen to a Cape Cod estuary, *Limnol. Oceanogr.*, 46, 465–470, 2001.

Charette, M. A., Splivallo, R., Herbold, C., Bollinger, M. S., and Moore, W. S.: Salt marsh submarine groundwater discharge as traced by radium isotopes, *Mar. Chem.*, 84, 113–121, 2003.

Charette, M. A., Moore, W. S., and Burnett, W. C.: Uranium-and thorium-series nuclides as tracers of submarine groundwater discharge, in: *U-Th series Nuclides in Aquatic systems*, edited by: Krishnaswami, S., Cochran, J. K., 13, Amsterdam, Elsevier, 155–191, 2008.

How significant is submarine groundwater discharge?

Q. Liu et al.

[Title Page](#)
[Abstract](#)
[Introduction](#)
[Conclusions](#)
[References](#)
[Tables](#)
[Figures](#)




[Back](#)
[Close](#)
[Full Screen / Esc](#)
[Printer-friendly Version](#)
[Interactive Discussion](#)


- Chen, W., Liu, Q., Huh, C.-A., Dai, M., and Miao, Y.-C.: Signature of the Mekong River plume in the western South China Sea revealed by radium isotopes, *J. Geophys. Res.*, 115, C12002, doi:10.1029/12010JC006460, 2010.
- Chen, Y.: Groundwater analysis in the watershed downstream of Hanjiang along the coast of Yue Dong, Guangdong water resources and hydropower, 31–32, 2008 (in Chinese).
- Dagg, M., Dai, M., Harrison, P., and Rabouille, C.: Introduction, *Cont. Shelf Res.*, 28, V-VI, 2008.
- Das, P., Marchesiello, P., and Middleton, J. H.: Numerical modelling of tide-induced residual circulation in Sydney Harbour, *Mar. Freshwater Res.*, 51, 97–112, 2000.
- Delhez, E. J. M., Deleersnijder, E., Mouchet, A., and Beckers, J.-M.: A note on the age of radioactive tracers, *J. Mar. Res.*, 38, 277–286, 2003.
- Dulaiova, H. and Burnett, W. C.: Are groundwater inputs into river-dominated areas important? The Chao Phraya River-Gulf of Thailand, *Limnol. Oceanogr.*, 51, 2232–2247, 2006.
- Gan, J., Li, L., Wang, D., and Guo, X.: Interaction of a river plume with coastal upwelling in the northeastern South China Sea, *Cont. Shelf Res.*, 29, 728–740, 2009a.
- Gan, J., Cheung, A. Y. Y., Guo, X., and Li, L.: Intensified upwelling over a widened shelf in the northeastern South China Sea, *J. Geophys. Res.*, 114, C09019, doi:09010.01029/02007JC004660, 2009b.
- Gan, J., Lu, Z., Dai, M., Cheung, A. Y. Y., Liu, H., and Harrison, P.: Biological response to intensified upwelling and to a river plume in the northeastern South China Sea: A modeling study, *J. Geophys. Res.*, 115, doi:10.1029/2009JC005569, 2010.
- Garcia-Solsona, E., Garcia-Orellana, J., Masque, P., and Dulaiova, H.: Uncertainties associated with Ra-223 and Ra-224 measurements in water via a Delayed Coincidence Counter (RaDeCC), *Mar. Chem.*, 109, 198–219, 2008.
- Garcia-Solsona, E., Garcia-Orellana, J., Masqué, P., Rodellas, V., Mejías, M., Ballesteros, B., and Domínguez, J. A.: Groundwater and nutrient discharge through karstic coastal springs (*Castell*, Spain), *Biogeosciences*, 7, 2625–2638, doi:10.5194/bg-7-2625-2010, 2010.
- Giffin, C., Kaufman, A., and Broecker, W.: Delayed coincidence counter for the assay of actinon and thoron, *J. Geophys. Res.*, 68, 1749–1757, 1963.
- Guo, X., Cai, W.-J., Zhai, W., Dai, M., Wang, Y., and Chen, B.: Seasonal variations in the inorganic carbon system in the Pearl River (Zhujiang) estuary, *Cont. Shelf Res.*, 28, 1424–1434, 2008.
- Han, A., Dai, M., Gan, J., Kao, S.-J., Li, Q., Wang, L., Zhai, W., Cai, P., and Huang, B.: Nutrient

How significant is submarine groundwater discharge?

Q. Liu et al.

Title Page

Abstract

Introduction

Conclusions

References

Tables

Figures

⏪

⏩

◀

▶

Back

Close

Full Screen / Esc

Printer-friendly Version

Interactive Discussion



dynamics in a large continental shelf system under the influence of both a river plume and coastal upwelling, *Limnol. Oceanogr.*, accepted, 2011.

Hancock, G. J., Webster, I. T., Ford, P. W., and Moore, W. S.: Using Ra isotopes to examine transport processes controlling benthic fluxes into a shallow estuarine lagoon, *Geochim. Cosmochim. Ac.*, 64, 3685–3699, 2000.

Hancock, G. J., Webster, I. T., and Stieglitz, T. C.: Horizontal mixing of Great Barrier Reef waters: Offshore diffusivity determined from radium isotope distribution, *J. Geophys. Res.*, 111, doi:10.1029/2006JC003608, 2006.

Hiroshi, N. and Emery, K. O.: Sediments of Shallow Portions of East China Sea and South China Sea, *Geol. Soc. Am. Bull.*, 72, 731–762, 1961.

Hu, C. M., Muller-Karger, F. E., and Swarzenski, P. W.: Hurricanes, submarine groundwater discharge, and Florida's red tides, *J. Geophys. Res.*, 33, doi:10.1029/2005GL025449, 2006.

Johannes, R. E.: The ecological significance of the submarine discharge of ground water, *Mar. Ecol. Prog. Ser.*, 3, 365–373, 1980.

Kelly, R. P. and Moran, S. B.: Seasonal changes in groundwater input to a well-mixed estuary estimated using radium isotopes and implications for coastal nutrient budgets, *Limnol. Oceanogr.*, 47, 1796–1807, 2002.

Kim, G., Kim, J.-S., and Hwang, D.-W.: Submarine groundwater discharge from oceanic islands standing in oligotrophic oceans: Implications for global biological production and organic carbon fluxes, *Limnol. Oceanogr.*, 56, 673–682, 2011.

Krest, J. M., Moore, W. S., and Rama: ^{226}Ra and ^{228}Ra in the mixing zones of the Mississippi and Atchafalaya Rivers: indicators of groundwater input, *Mar. Chem.*, 64, 129–154, 1999.

Lee, Y. W., and Kim, G.: Linking groundwater-borne nutrients and dinoflagellate red-tide outbreaks in the southern sea of Korea using a Ra tracer, *Estuar. Coast. Shelf S.*, 71, 309–317, 2007.

Lee, Y. W., Kim, G., Lim, W. A., and Hwang, D. W.: A relationship between submarine groundwater-borne nutrients traced by Ra isotopes and the intensity of dinoflagellate red-tides occurring in the southern sea of Korea, *Limnol. Oceanogr.*, 55, 1–10, 2010.

Li, Y.-H., Mathieu, G., Biscaye, P., and Simpson, H. J.: The flux of ^{226}Ra from estuarine and continental shelf sediments, *Earth Planet. Sci. Lett.*, 37, 237–241, 1977.

Liao, X. Y., Liang, J., Lao, W. B., Zhou, M. X., and Liu, H. D. : In: *Groundwater Resources of China-Guangdong Province*, edited by: Zhang Z. and Li L., The Map of China Publishing House, Beijing, China, 81 pp., 2005 (in Chinese).

**How significant is
submarine
groundwater
discharge?**

Q. Liu et al.

[Title Page](#)[Abstract](#)[Introduction](#)[Conclusions](#)[References](#)[Tables](#)[Figures](#)[⏪](#)[⏩](#)[◀](#)[▶](#)[Back](#)[Close](#)[Full Screen / Esc](#)[Printer-friendly Version](#)[Interactive Discussion](#)

Liu, G.-S., Huang, Yi-Pu, Chen, M., Qiu, Y.-S., Cai, Y.-H., and Gao, Z.-Y.: Specific activity and distribution of natural radionuclides and ^{137}Cs in surface sediments of the northeastern South China Sea, *Acta Oceanologica Sinica*, 23, 76–84, 2001 (in Chinese).

Luo, Y., Lao, H., and Wang, L.: A preliminary study on the surface sediment types and their grain size characteristics of the northeastern part of the South China Sea, *Tropical Oceanology*, 4, 33–41, 1985 (in Chinese).

Marsh, J. A.: Terrestrial inputs of nitrogen and phosphorus on fringing reefs of Guam, in: *Proceedings of the 2nd International Coral Reef Symposium, I*, Great Barrier Reef Committee, Brisbane, Australia, 332–336, 1977.

Moore, W. S.: Sampling ^{228}Ra in the deep ocean, *Deep Sea Res.*, 23, 647–651, 1976.

Moore, W. S.: Radium isotope measurements using germanium detectors, *Nucl. Instrum Meth B.*, 223, 407–411, 1984.

Moore, W. S.: Ages of continental shelf waters determined from ^{223}Ra and ^{224}Ra , *J. Geophys. Res.*, 105(C9), 22117–22122, 2000a.

Moore, W. S.: Determining coastal mixing rates using radium isotopes, *Cont. Shelf Res.*, 20, 1993–2007, 2000b.

Moore, W. S.: Sources and fluxes of submarine groundwater discharge delineated by radium isotopes, *Biogeochemistry*, 66, 75–93, 2003.

Moore, W. S.: Radium isotopes as tracers of submarine groundwater discharge in Sicily, *Cont. Shelf Res.*, 26, 852–861, 2006.

Moore, W. S.: Seasonal distribution and flux of radium isotopes on the southeastern US continental shelf, *J. Geophys. Res.*, 112, C10013, doi:10.1029/2007JC004199, 2007.

Moore, W. S.: Fifteen years experience in measuring ^{224}Ra and ^{223}Ra by delayed-coincidence counting, *Mar. Chem.*, 109, 188–197, 2008.

Moore, W. S.: The Effect of Submarine Groundwater Discharge on the Ocean, *Annu. Rev. Mar. Sci.*, 2, 59–88, 2010a.

Moore, W. S.: A reevaluation of submarine groundwater discharge along the southeastern coast of North America, *Global Biogeochem. Cy.*, 24, GB4005, doi:10.1029/2009GB003747, 2010b.

Moore, W. S. and Arnold, R.: Measurement of ^{223}Ra and ^{224}Ra in coastal waters using a delayed coincidence counter, *J. Geophys. Res.*, 101, 1321–1329, 1996.

Moore, W. S. and Krest, J.: Distribution of ^{223}Ra and ^{224}Ra in the plumes of the Mississippi and Atchafalaya Rivers and the Gulf of Mexico, *Mar. Chem.*, 86, 105–119, 2004.

How significant is submarine groundwater discharge?

Q. Liu et al.

Title Page

Abstract

Introduction

Conclusions

References

Tables

Figures

⏪

⏩

◀

▶

Back

Close

Full Screen / Esc

Printer-friendly Version

Interactive Discussion

- Moore, W. S., Key, R. M., and Sarmiento, J. L.: Techniques for precise mapping of ^{226}Ra and ^{228}Ra in the ocean, *J. Geophys. Res.*, 90, 6983–6994, 1985.
- Moore, W. S., Blanton, J. O., and Joye, S. B.: Estimates of flushing times, submarine groundwater discharge, and nutrient fluxes to Okatee Estuary, South Carolina, *J. Geophys. Res.*, 111, C09006, doi:10.1029/2005JC003041, 2006.
- Moore, W. S., Sarmiento, J. L., and Key, R. M.: Submarine groundwater discharge revealed by Ra-228 distribution in the upper Atlantic Ocean, *Nat. Geosci.*, 1, 309–311, 2008.
- Mulligan, A. E. and Charette, M. A.: Intercomparison of submarine groundwater discharge estimates from a sandy unconfined aquifer, *J. Hydrol.*, 327, 411–425, 2006.
- Pilson, M. E. Q.: On the residence time of water in Narragansett Bay, *Estuaries*, 8, 2–14, 1985.
- Rasmussen, L. L.: Radium Isotopes as Tracers of Coastal Circulation Pathways in the Mid-Atlantic Bight, Ph.D. thesis, Massachusetts Institute of Technology Woods Hole Oceanographic Institution, Woods Hole, Massachusetts, 214 pp., 2003.
- Sanford, L., Boicourt, W., and Rives, S.: Model for estimating tidal flushing of small embayments, *J. Waterw. Port C.*, 118, 635–654, 1992.
- Santos, I. R., Burnett, W. C., Chanton, J., Mwashote, B., Suryaputra, I. G. N. A., and Dittmar, T.: Nutrient biogeochemistry in a Gulf of Mexico subterranean estuary and groundwater-derived fluxes to the coastal ocean, *Limnol. Oceanogr.*, 53, 705–718, 2008.
- Shu, Y. Q., Wang, D. X., Zhu, J., and Peng, S. Q.: The 4-D structure of upwelling and Pearl River plume in the northern South China Sea during summer 2008 revealed by a data assimilation model, *Ocean Model.*, 36, doi:10.1016/j.ocemod.2011.01.002, 2011a.
- Shu, Y. Q., Zhu, J., Wang, D. X., and Xiao, X. J.: Assimilating remote sensing and in situ observations into a coastal model of northern South China Sea using ensemble Kalman filter, *Cont. Shelf Res.*, 31, S24–S36, 2011b.
- Slomp, C. P. and Van Cappellen, P.: Nutrient inputs to the coastal ocean through submarine groundwater discharge: controls and potential impact, *J. Hydrol.*, 295, 64–86, 2004.
- Stalker, J. C., Price, R. M., and Swart, P. K.: Determining Spatial and Temporal Inputs of Freshwater, Including Submarine Groundwater Discharge, to a Subtropical Estuary Using Geochemical Tracers, Biscayne Bay, South Florida, *Estuaries. Coasts*, 32, 694–708, 2009.
- Striegl, R. G. and Michmerhuizen, C. M.: Hydrologic influence on methane and carbon dioxide dynamics at two north-central Minnesota lakes, *Limnol. Oceanogr.*, 43, 1519–1529, 1998.
- Swarzenski, P. W., Reich, C. D., Spechler, R. M., Kindinger, J. L., and Moore, W. S.: Using multiple geochemical tracers to characterize the hydrogeology of the submarine spring off

- Crescent Beach, Florida, Chem. Geol., 179, 187–202, 2001.
- Taniguchi, M., Burnett, W. C., Cable, J. E., and Turner, J. V.: Investigation of submarine ground-water discharge, Hydrol. Process., 16, 2115–2129, 2002.
- 5 Zhang, F., Zhang, W., and Yang, Q.: Characteristics of grain size distributions of surface sediments in the eastern south china sea, Acta Sedimentologica Sinica, 21, 452–460, 2003 (in Chinese).

BGD

8, 12381–12422, 2011

How significant is submarine groundwater discharge?

Q. Liu et al.

Title Page

Abstract

Introduction

Conclusions

References

Tables

Figures



Back

Close

Full Screen / Esc

Printer-friendly Version

Interactive Discussion



Table 1. Activities of Ra isotopes at the sampling sites[#] on the Northern South China Sea shelf and in the Pearl River estuary.

Sample ID	Latitude (° N)	Longitude (° E)	Salinity	ex ²²⁴ Ra*	²²³ Ra	²²⁶ Ra (dpm 100 L ⁻¹)	²²⁸ Ra
Northern South China Sea							
S106	21.80	115.20	29.1	11.39 ± 0.52	1.13 ± 0.11	20.18 ± 1.23	55.55 ± 2.50
S110	21.22	115.80	33.8	2.86 ± 0.16	0.03 ± 0.02	7.59 ± 0.49	12.74 ± 1.39
S209	21.51	115.75	33.7	2.62 ± 0.15	0.07 ± 0.02	5.15 ± 0.80	7.10 ± 0.91
S207	21.84	115.67	33.3	2.92 ± 0.19	0.06 ± 0.02	8.22 ± 0.87	7.96 ± 1.46
S206	22.00	115.63	33.4	5.11 ± 0.31	0.53 ± 0.06	10.46 ± 1.45	28.17 ± 3.36
S205	22.15	115.59	30.8	8.61 ± 0.38	1.05 ± 0.09	18.40 ± 2.22	40.20 ± 3.31
S204	22.30	115.55	30.1	5.09 ± 0.32	0.73 ± 0.07	20.95 ± 1.62	35.00 ± 4.55
S203	22.40	115.53	28.5	5.25 ± 0.31	0.97 ± 0.08	12.66 ± 1.54	40.31 ± 2.61
S202	22.50	115.50	30.8	8.17 ± 0.37	0.91 ± 0.08	22.84 ± 2.90	45.10 ± 4.67
S201	22.58	115.48	29.6	13.26 ± 0.51	0.96 ± 0.12	16.49 ± 1.60	41.25 ± 2.48
S201-7 m	22.58	115.48	32.1	7.56 ± 0.42	0.59 ± 0.08	17.19 ± 3.84	45.29 ± 4.16
S201-15 m	22.58	115.48	34.1	17.63 ± 0.95	1.38 ± 0.18	11.42 ± 0.76	35.60 ± 3.27
S305	22.16	116.18	32.4	25.94 ± 0.87	0.59 ± 0.08	17.19 ± 3.84	45.29 ± 4.16
S305-10 m	22.16	116.18	33.0	0.25 ± 0.14	1.38 ± 0.18	11.42 ± 0.76	35.60 ± 3.27
S305-25 m	22.16	116.18	33.8	0.28 ± 0.17	1.69 ± 0.21	8.27 ± 0.78	27.94 ± 2.72
S305-45 m	22.16	116.18	34.1	0.23 ± 0.12	0.03 ± 0.02	9.37 ± 1.46	7.43 ± 3.12
S305-60 m	22.16	116.18	34.4	1.78 ± 0.20	0.13 ± 0.03	7.62 ± 0.88	14.40 ± 1.45
S306	22.00	116.26	33.7	0.25 ± 0.14	0.03 ± 0.02	9.37 ± 1.46	7.43 ± 3.12
S308	21.70	116.43	33.8	0.31 ± 0.15	0.03 ± 0.03	7.87 ± 0.67	6.85 ± 1.21
S310	21.41	116.64	33.8	0.01 ± 0.14	0.02 ± 0.01	9.11 ± 0.82	15.30 ± 1.50
S409	21.80	117.20	33.4	0.09 ± 0.11	0.03 ± 0.02	15.36 ± 1.89	16.00 ± 2.08
S407	22.10	116.90	33.3	3.76 ± 0.26	0.94 ± 0.09	16.33 ± 0.84	54.62 ± 2.40
S406	22.25	116.75	32.4	4.51 ± 0.34	0.74 ± 0.08	27.88 ± 2.30	52.66 ± 3.16
S405	22.35	116.65	32.0	1.24 ± 0.19	0.42 ± 0.05	15.14 ± 1.26	33.62 ± 2.38
S404	22.45	116.55	30.4	2.93 ± 0.29	0.72 ± 0.08	12.75 ± 1.65	31.08 ± 4.34
S403	22.55	116.45	32.4	7.81 ± 0.43	0.89 ± 0.09	15.72 ± 1.46	34.64 ± 3.38
S402	22.65	116.34	32.6	10.31 ± 0.51	1.37 ± 0.11	15.66 ± 3.84	48.08 ± 5.35
S401	22.75	116.29	33.4	29.15 ± 1.11	1.51 ± 0.16	10.14 ± 1.52	40.06 ± 4.18
S401-b	22.90	116.67	34.0	10.21 ± 0.46	0.86 ± 0.10	6.57 ± 0.66	16.70 ± 1.82
S501	23.10	116.90	33.9	19.01 ± 0.61	1.21 ± 0.12	16.02 ± 0.99	–
S503	22.90	117.10	29.5	17.21 ± 0.42	1.94 ± 0.15	15.79 ± 1.01	55.31 ± 2.73
S504	22.80	117.20	31.6	4.35 ± 0.31	0.88 ± 0.10	18.11 ± 2.55	42.07 ± 4.37
S505	22.69	117.30	29.4	4.35 ± 0.31	0.72 ± 0.08	22.49 ± 2.47	41.41 ± 5.16
S506	22.59	117.40	27.1	2.56 ± 0.27	0.80 ± 0.08	18.74 ± 1.44	51.49 ± 2.61
S508	22.30	117.70	30.9	2.87 ± 0.27	0.71 ± 0.09	18.70 ± 2.18	55.38 ± 4.07
S510	22.00	118.00	33.0	0.01 ± 0.11	0.03 ± 0.01	7.61 ± 0.41	8.43 ± 1.09
S608	22.30	118.20	33.0	0.01 ± 0.11	0.07 ± 0.03	9.83 ± 0.77	12.91 ± 1.67
S606	22.60	117.90	32.7	1.06 ± 0.23	0.26 ± 0.06	12.18 ± 0.95	29.05 ± 2.10

How significant is submarine groundwater discharge?

Q. Liu et al.

Title Page

Abstract

Introduction

Conclusions

References

Tables

Figures

◀

▶

◀

▶

Back

Close

Full Screen / Esc

Printer-friendly Version

Interactive Discussion



How significant is submarine groundwater discharge?

Q. Liu et al.

Title Page

Abstract

Introduction

Conclusions

References

Tables

Figures

◀

▶

◀

▶

Back

Close

Full Screen / Esc

Printer-friendly Version

Interactive Discussion



Table 1. Continued.

Sample ID	Latitude (° N)	Longitude (° E)	Salinity	ex ²²⁴ Ra	²²³ Ra	²²⁶ Ra (dpm 100L ⁻¹)	²²⁸ Ra
S605	22.75	117.75	31.3	2.78 ± 0.28	1.19 ± 0.09	21.69 ± 2.55	55.67 ± 5.41
S604	22.90	117.60	31.0	3.52 ± 0.31	0.99 ± 0.09	24.05 ± 2.62	53.69 ± 5.08
S603	23.05	117.45	29.4	4.84 ± 0.27	1.38 ± 0.10	19.21 ± 1.93	47.31 ± 3.32
S602	23.20	117.30	32.2	18.71 ± 0.28	1.22 ± 0.15	24.89 ± 3.37	41.15 ± 3.43
S601	23.30	117.45	33.6	9.46 ± 0.29	0.49 ± 0.05	15.08 ± 1.85	15.76 ± 1.89
S701	23.51	117.49	33.8	43.99 ± 0.94	1.70 ± 0.19	9.98 ± 1.53	29.15 ± 2.45
S702	23.45	117.55	33.9	11.19 ± 0.46	0.40 ± 0.07	10.76 ± 1.60	12.38 ± 2.91
S702-15m	23.45	117.55	33.9	6.77 ± 0.37	0.25 ± 0.06	8.14 ± 1.47	16.67 ± 1.73
S702-35m	23.45	117.55	33.9	9.89 ± 0.49	0.30 ± 0.08	10.65 ± 1.09	16.05 ± 2.16
S703	23.35	117.65	33.3	8.88 ± 0.69	0.32 ± 0.10	7.79 ± 0.90	14.92 ± 1.95
S705	23.10	117.90	31.3	7.01 ± 0.65	0.35 ± 0.09	8.13 ± 1.46	16.66 ± 1.72
S707	22.80	118.20	32.6	10.85 ± 0.34	0.57 ± 0.06	14.40 ± 1.39	28.75 ± 1.98
S709	22.51	118.51	29.9	0.19 ± 0.16	0.35 ± 0.03	15.94 ± 1.71	34.96 ± 2.15
Pearl River Estuary							
6	22.12	114.44	24.6	37.17 ± 0.62	2.04 ± 0.21	21.18 ± 1.31	51.89 ± 4.77
A	21.67	114.05	27.0	4.53 ± 0.54	0.43 ± 0.11	14.80 ± 0.85	35.85 ± 2.78
B	21.73	113.94	23.5	7.60 ± 0.92	0.84 ± 0.60	20.44 ± 1.28	57.07 ± 4.93
C	21.96	113.86	16.7	22.77 ± 1.61	1.73 ± 0.81	22.76 ± 1.69	70.62 ± 4.32
D	22.03	113.86	12.1	34.57 ± 1.77	2.35 ± 0.88	29.83 ± 1.58	75.23 ± 4.66
E	22.37	113.78	10.2	51.14 ± 2.51	2.56 ± 1.09	19.67 ± 2.11	60.82 ± 6.83
F	22.44	113.76	7.4	63.31 ± 4.27	1.35 ± 0.82	30.74 ± 1.66	66.19 ± 3.37
G	22.61	113.71	6.0	39.42 ± 1.35	0.80 ± 0.74	23.76 ± 2.12	48.08 ± 4.97
H	22.71	113.68	5.4	32.32 ± 1.87	0.87 ± 0.88	14.97 ± 1.44	35.36 ± 3.70
I	23.11	113.31	5.1	31.80 ± 1.94	1.38 ± 0.59	23.60 ± 2.05	27.59 ± 7.15

* ex²²⁴Ra denotes excess ²²⁴Ra, corrected for the ingrowth from ²²⁸Th;

Ra isotopes profiling was only sampled at stations S201, S305 and S702 and only surface water was collected at the rest of the stations.

How significant is submarine groundwater discharge?

Q. Liu et al.

Table 2. Submarine Groundwater discharge (SGD) estimated based on a three end-member mixing model and Ra mass balance in the Northern South China Sea. Also shown are the sensitivity analysis and error sources with different methods.

Method		SGD $10^7 \text{ m}^3 \text{ d}^{-1}$	Error Source		Uncertainty (%)
Three end-member mixing model	^{228}Ra and TAlk	23 ± 28	Ra end-member	groundwater river plume offshore	3.6–3.8* 6.3–7.1* 1.3–3.1*
	^{226}Ra and TAlk	37 ± 46	TAlk end-member	groundwater river plume offshore	6.0–7.5* 59.5–72.5* 59.6–75.2*
Ra Mass	^{226}Ra with upwelling	33 ± 68	Ra end-member	groundwater river plume offshore	4.8* 15.5–44.1* 19.3–27.6*
	^{228}Ra with upwelling	45 ± 56		upwelling	3.6–4.1*
Balance	^{228}Ra without upwelling	28 ± 43	Mixed layer depth Water age		0.1–2.7 (depth changes 1 m) 20.6–25.9 (varying 1 day)
	^{226}Ra without upwelling	39 ± 53	Upwelling rate		4.0*

* represents 5% variation with each error source.

Title Page

Abstract

Introduction

Conclusions

References

Tables

Figures

⏪

⏩

◀

▶

Back

Close

Full Screen / Esc

Printer-friendly Version

Interactive Discussion



How significant is submarine groundwater discharge?

Q. Liu et al.

Table 3. Definitions and values used for ²²⁶Ra and ²²⁸Ra mass balance to estimate submarine groundwater discharge flux to the northern South China Sea.

	Definition	²²⁶ Ra	²²⁸ Ra	Unit
Ra _{Riv}	Pearl River Plume end-member	29.83 ± 1.58	75.24 ± 4.66	dpm 100 L ⁻¹
Ra _{Gw}	Average activity of Ra in the groundwater	207.48 ± 11.11	531.80 ± 15.21	dpm 100 L ⁻¹
Ra _{Off}	Ra activity in the offshore surface water	5.15 ± 0.80	7.10 ± 0.92	dpm 100 L ⁻¹
τ	Water age	16 ± 10 [*]		days
		14 ± 10 [#]		
F _{Riv}	Discharge of the Pearl River	1.76 × 10 ⁹		m ³ d ⁻¹
A _{Sed}	Surface area of benthic sediment	3.08 × 10 ¹⁰		m ²
Ra _{Sed}	Diffusive benthic flux of Ra	0.45	25	dpm m ⁻² d ⁻¹
H	Mixed layer depth	5–30		m
Ra _{Uw}	Average activity of Ra in the subsurface offshore water	8.26 ± 0.78	27.94 ± 2.72	dpm 100 L ⁻¹
A _{Uw}	Surface area of the upwelling zone	1.99 × 10 ⁹		m ²
v	Upwelling rate	1.7		m d ⁻¹

* represents no upwelling; # denotes with upwelling.

Title Page

Abstract

Introduction

Conclusions

References

Tables

Figures

⏪

⏩

◀

▶

Back

Close

Full Screen / Esc

Printer-friendly Version

Interactive Discussion



How significant is submarine groundwater discharge?

Q. Liu et al.

Title Page

Abstract

Introduction

Conclusions

References

Tables

Figures

⏪

⏩

◀

▶

Back

Close

Full Screen / Esc

Printer-friendly Version

Interactive Discussion



Table 4. Fractional contributions of various sources to the total ^{226}Ra and ^{228}Ra flux into the northern South China Sea.

Method	River	Sediment	Groundwater	Upwelling
	Dissolved Ra + suspended particles release			
^{228}Ra Box(NU)	36 %	21 %	42 %	–
^{226}Ra Box(NU)	50 %	2 %	48 %	–
^{228}Ra Box(WU)	26 %	16 %	38 %	20 %
^{226}Ra Box(WU)	36 %	1 %	43 %	20 %

NU represents no upwelling; WU denotes with upwelling.

How significant is submarine groundwater discharge?

Q. Liu et al.

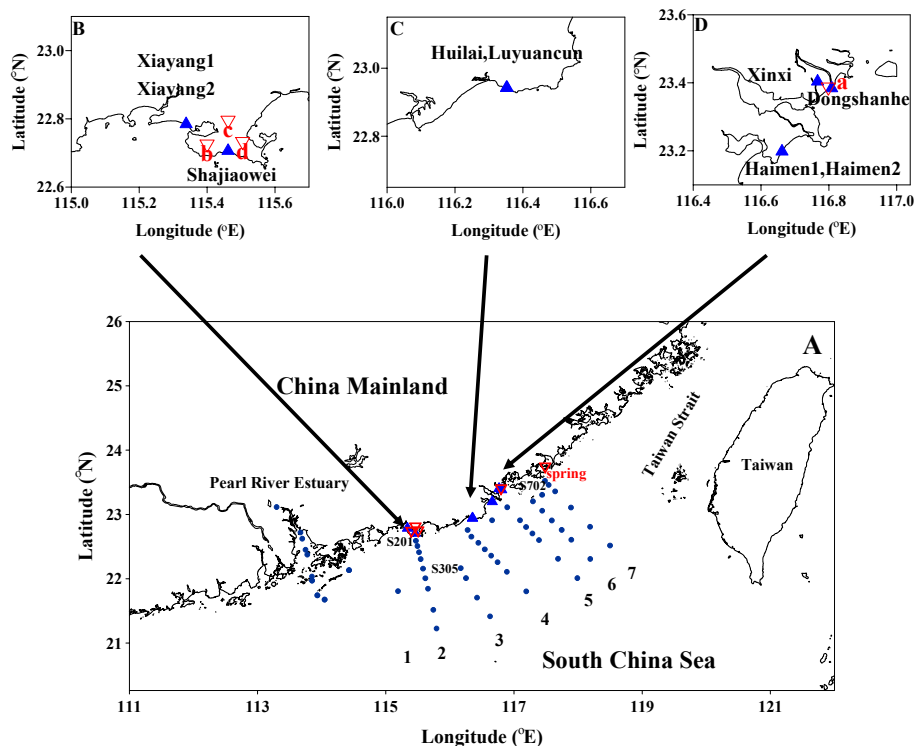


Fig. 1. Map of the northern South China Sea showing the sampling sites (A) occupied during 30 June–8 July, 2008 and the sites for groundwater sampling along the coast (B, C, D). Blue dots represent Ra samples on the surface water, the cross-shelf transects are marked by numbers 1–7. Solid triangle and open inverted triangle indicate groundwater samples collected in December 2008 and October 2010, respectively.

How significant is submarine groundwater discharge?

Q. Liu et al.

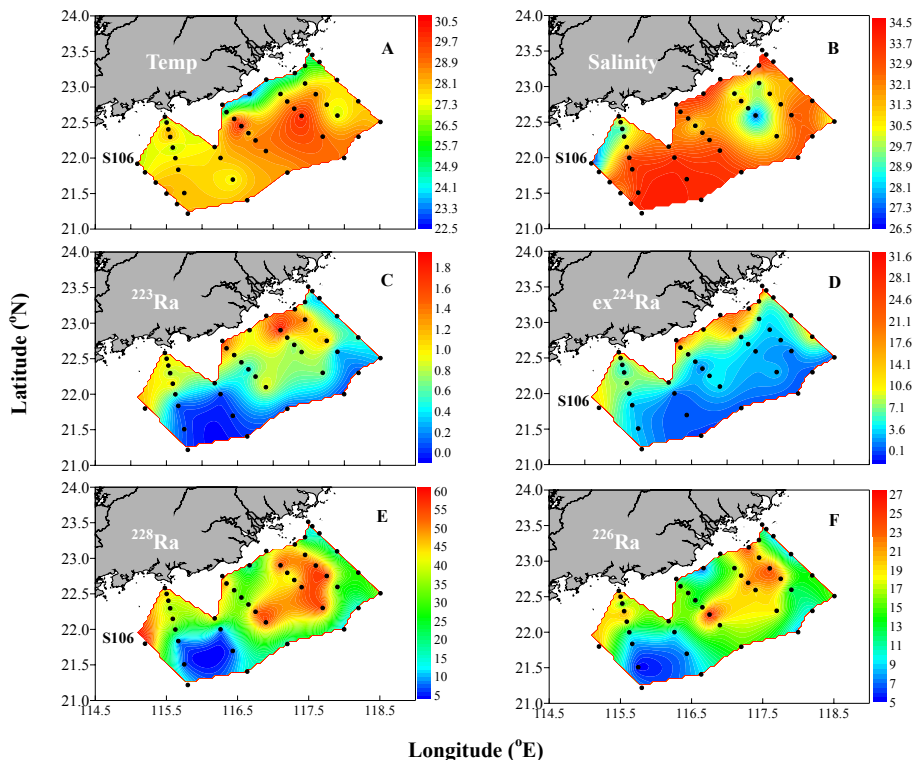


Fig. 2. Contour maps of distributions of **(A)** temperature (°C), **(B)** salinity, **(C)** ^{223}Ra (dpm 100 L⁻¹), **(D)** ex ^{224}Ra (excess ^{224}Ra , corrected for the ingrowth from ^{228}Th ; dpm 100 L⁻¹), **(E)** ^{228}Ra (dpm 100 L⁻¹), and **(F)** ^{226}Ra (dpm 100 L⁻¹) in the northern South China Sea during 30 June–8 July, 2008.

Title Page

Abstract Introduction

Conclusions References

Tables Figures

◀ ▶

◀ ▶

Back Close

Full Screen / Esc

Printer-friendly Version

Interactive Discussion

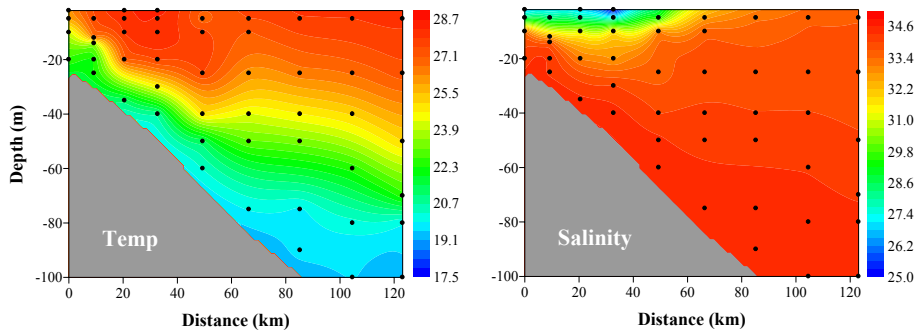


Fig. 3. Temperature ($^{\circ}\text{C}$) and salinity at the cross-shelf transect 2 in the northern South China Sea.

How significant is submarine groundwater discharge?

Q. Liu et al.

Title Page

Abstract Introduction

Conclusions References

Tables Figures

⏪ ⏩

◀ ▶

Back Close

Full Screen / Esc

Printer-friendly Version

Interactive Discussion



How significant is submarine groundwater discharge?

Q. Liu et al.

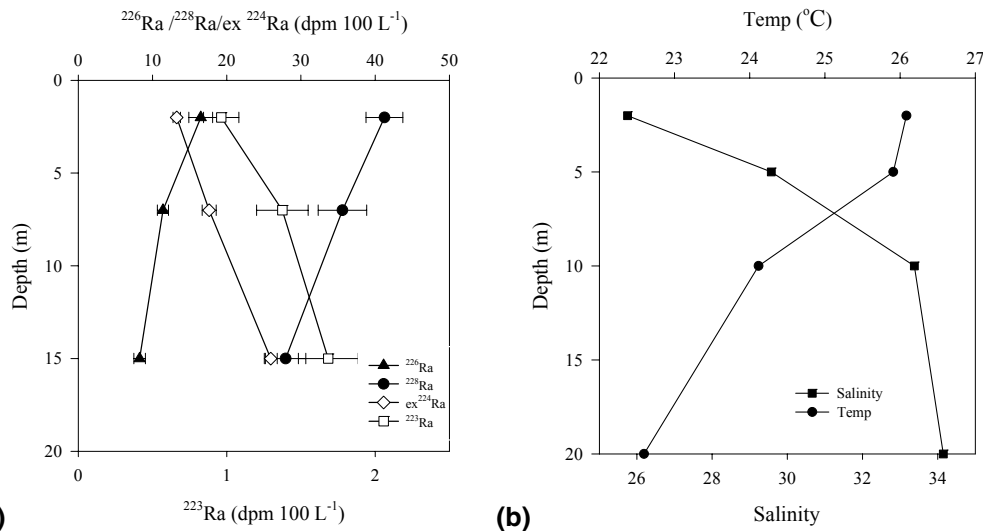


Fig. 4. Vertical profiles of ^{226}Ra , ^{228}Ra , ex ^{224}Ra (excess ^{224}Ra , corrected for the ingrowth from ^{228}Th), and ^{223}Ra (a) and temperature and salinity (b) at S201 located at the nearest to the shore at Transect 2.

How significant is submarine groundwater discharge?

Q. Liu et al.

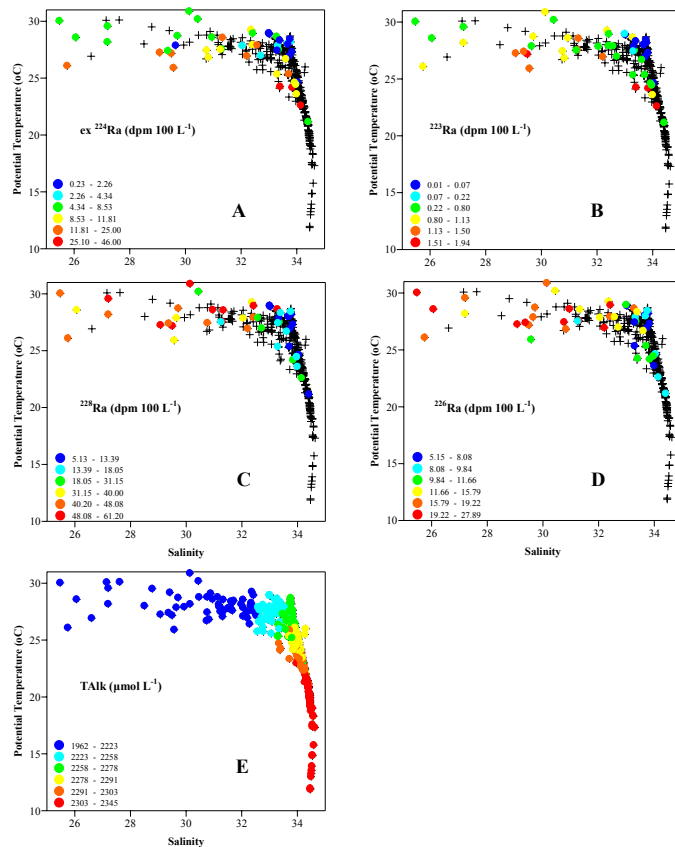


Fig. 5. Temperature-salinity diagrams superimposed with data of (A) $ex\ ^{224}\text{Ra}$ (excess ^{224}Ra , corrected for the ingrowth from ^{228}Th), (B) ^{223}Ra , (C) ^{228}Ra , (D) ^{226}Ra , (E) TALK (total alkalinity) for samples collected in the northern South China Sea during 30 June–8 July, 2008.

How significant is submarine groundwater discharge?

Q. Liu et al.

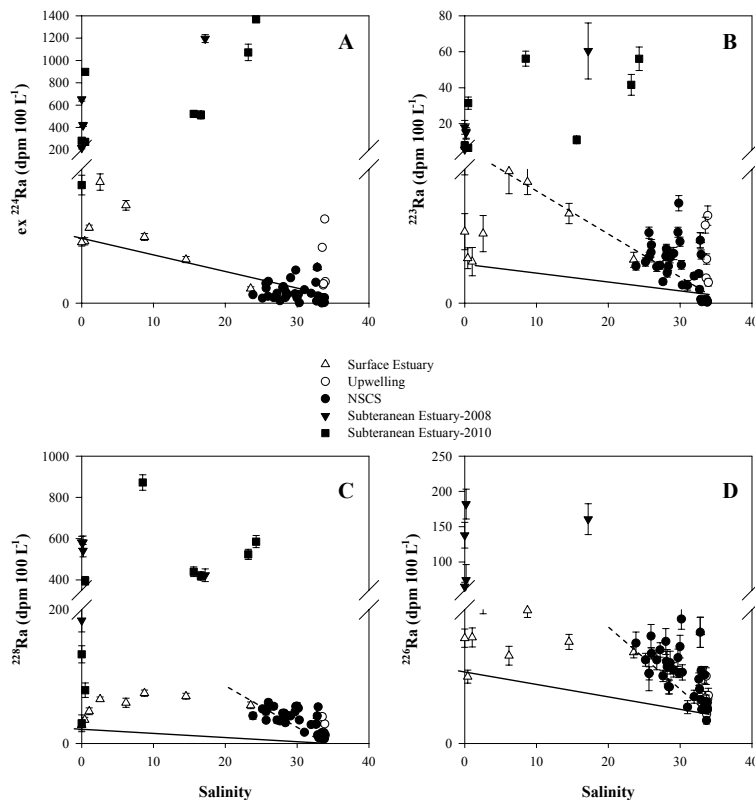


Fig. 6. Plots of (A) $\text{ex } ^{224}\text{Ra}$ (excess ^{224}Ra , corrected for the ingrowth from ^{228}Th), (B) ^{223}Ra , (C) ^{228}Ra , and (D) ^{226}Ra versus salinity in the estuary, subterranean estuary and northern South China Sea (NSCS) waters.

Title Page

Abstract

Introduction

Conclusions

References

Tables

Figures

◀

▶

◀

▶

Back

Close

Full Screen / Esc

Printer-friendly Version

Interactive Discussion

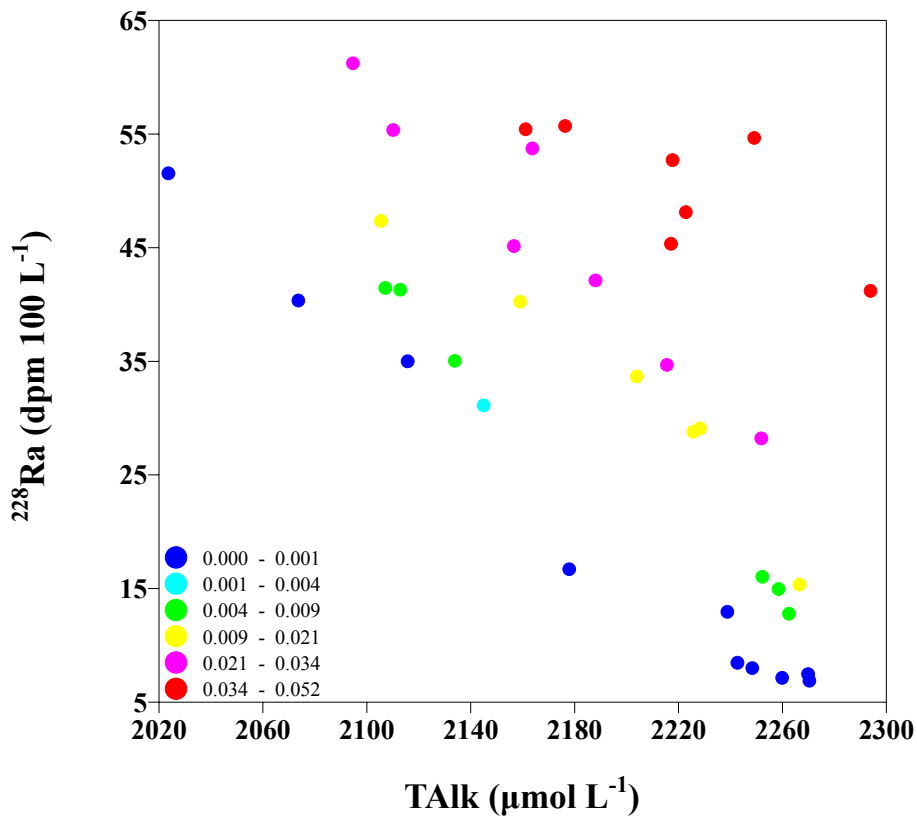


Fig. 7. ^{228}Ra and total alkalinity (TALK) diagram superimposed with the data of f (groundwater fraction) calculated based on the ^{228}Ra -TALK mixing model (for the period 30 June–8 July, 2008).

How significant is submarine groundwater discharge?

Q. Liu et al.

Title Page

Abstract Introduction

Conclusions References

Tables Figures

⏪ ⏩

◀ ▶

Back Close

Full Screen / Esc

Printer-friendly Version

Interactive Discussion



How significant is submarine groundwater discharge?

Q. Liu et al.

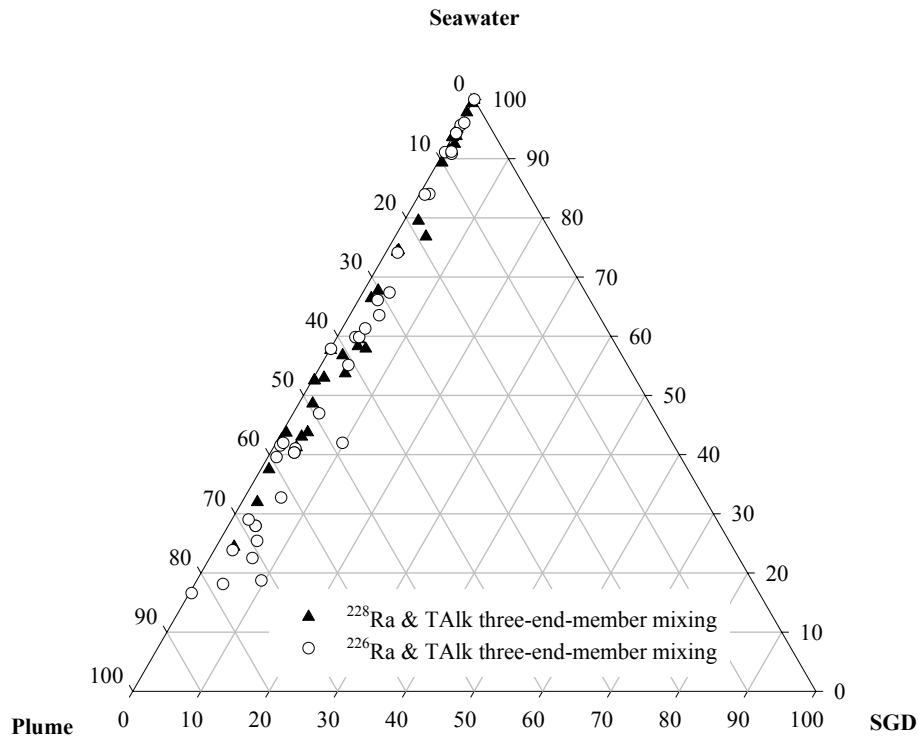


Fig. 8. Ternary diagram illustrating simulated percentage contributions from submarine groundwater discharge (SGD), offshore surface water, and Pearl River plume for surface water of the northern South China Sea for the period 30 June–8 July, 2008 using a three end-member mixing model based on ^{228}Ra and total alkalinity (TALK), and ^{226}Ra -TALK.

Title Page

Abstract

Introduction

Conclusions

References

Tables

Figures

◀

▶

◀

▶

Back

Close

Full Screen / Esc

Printer-friendly Version

Interactive Discussion

How significant is submarine groundwater discharge?

Q. Liu et al.

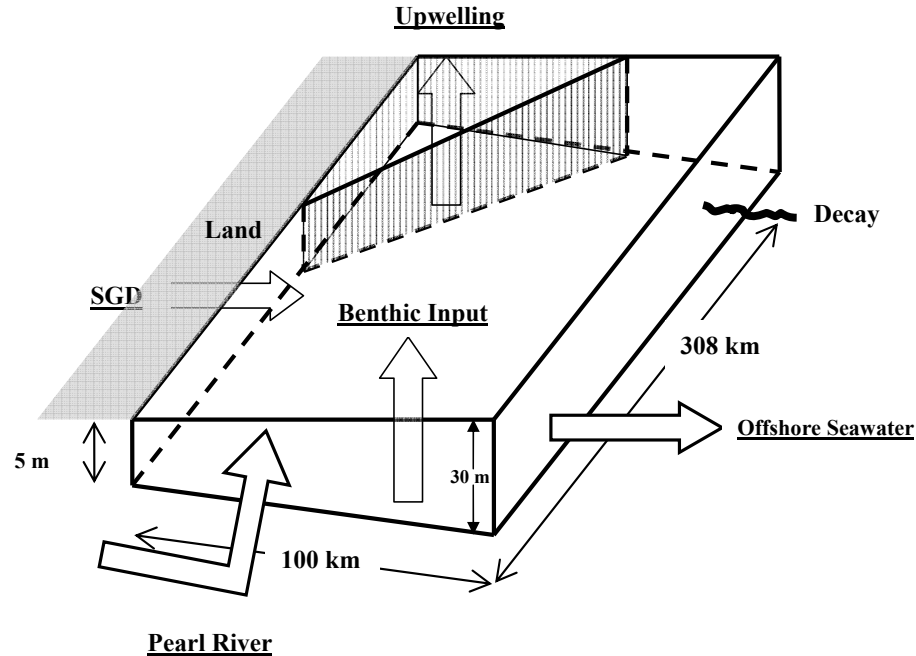


Fig. 9. Schematic of a box model for ^{228}Ra and ^{226}Ra balance in the northern South China Sea, which mainly covered seven cross-shelf transects with 308 km shoreline, 100 km offshore, mixed layer varied from 5 to 30 m. Sources of Ra include Pearl River, suspended particles re-release from Pearl River, benthic input, coastal upwelling and submarine groundwater discharge (SGD).